LANGMUIR Cite This: *Langmuir* 2019, 35, 824−830 Article pubs.acs.org/Langmuir

Modulation of Cu^{2+} Binding to Sphingosine-1-Phosphate by Lipid Charge

Alexis J. Baxter,[†] Adriana N. Santiago-Ruiz,[‡] Tinglu Yang,[†] and Paul S. Cremer*[,†,§]

[†]Department of Chemistry and [§]Department of Biochemistry and Molecular Biology, The Pennsylvania State University, University Park, Pennsylvania 16802, United States

[‡]Department of Chemistry, The University of Puerto Rico, Cayey, Puerto Rico 00736, United States

Supporting Information

ABSTRACT: Sphingosine-1-phosphate (S1P) is a sphingolipid metabolite that is thought to participate in the regulation of many physiological processes and may play a key role in several diseases. Herein, we found that Cu^{2+} binds tightly to supported lipid bilayers (SLBs) containing S1P. Specifically, we demonstrated via fluorescence assays that Cu^{2+}−S1P binding was bivalent and sensitive to the concentration of S1P in the SLB. In fact, the apparent equilibrium dissociation constant, K_{DApp}, tightened by a factor of 132 from 4.5 μM to 34 nM as the S1P density was increased from 5.0 to 20 mol %. A major driving force for this apparent tightening was the more negative surface potential with increasing S1P concentration. This potential remained unaltered upon Cu^{2+} binding at pH 7.4 because two protons were released for every Cu^{2+} that bound. At pH 5.4, however, Cu^{2+} could not outcompete protons for the amine and no binding occurred. Moreover, at pH 9.4, the amine was partially deprotonated before Cu^{2+} binding and the surface potential became more positive on binding. The results for Cu^{2+}−S1P binding were reminiscent of those for Cu^{2+}−phosphatidylserine binding, where a carboxylate group helped to deprotonate the amine. In the case of S1P, however, the phosphate needed to bear two negative charges to facilitate amine deprotonation in the presence of Cu^{2+}.

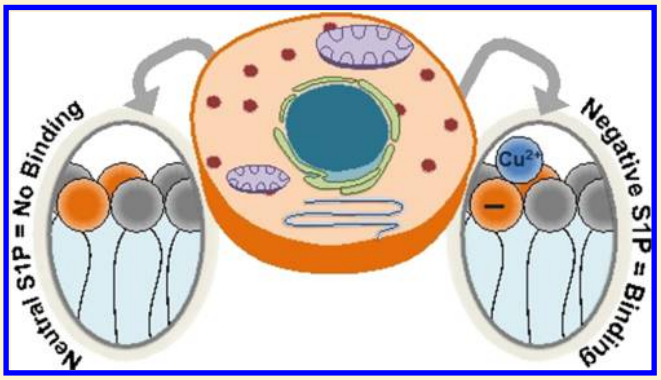

INTRODUCTION

Cations are known to interact with phospholipid headgroups and play important roles in numerous physiological processes. Such interactions have been shown to affect membrane surface charge, protein association, signaling cascades, and lipid domain formation.[1−6] The importance of metal ion−lipid interactions has been recognized for decades with many studies focusing on the interactions of Ca^{2+} and Mg^{2+} with negatively charged lipid vesicles.[7−11] These studies indicate that alkali metal cations have a dissociation constant of ∼10 mM for phosphatidylserine (PS) or phosphatidylglycerol (PG) lipids.[3] Other divalent metal ions, however, can show much tighter binding than Ca^{2+} and Mg^{2+}, depending on the headgroup chemistry. For example, divalent transition-metal ions can bind to both negatively charged and zwitterionic bilayers with apparent dissociation constants in the low pM range when amine moieties are present.[12−14]

Sphingosine-1-phosphate (S1P) is a single-tail lipid with a high plasma concentration that can easily insert into the outer membrane leaflet.[15−17] The structure of this molecule is shown in Figure 1a (left side). S1P, which is involved in the regulation of numerous physiological processes, is known to regulate cell growth and suppresses apoptosis. This suggests its potential involvement in the pathogenesis of cancer and inflammation disorders, such as asthma, osteoarthritis, and Alzheimer's disease.[18−21] S1P promotes cell survival in peripheral tissues, but excess S1P can be toxic to neurons.[22,23] The effects of S1P signaling have been evaluated in cellular assays by using primary neurons and neuronal cell lines.[24] Although some studies have explored S1P in vesicles,[25−27] very few have examined the behavior of S1P in supported model membrane systems, so little is known about the specific ion binding effects in bilayers with this lipid. Nevertheless, this molecule contains a primary amine and a phosphate moiety, which suggests that it should form complexes with first row transition-metal ions according to the Irving−Williams series.[28]

We demonstrate herein that S1P binds to Cu^{2+} in fluid-supported lipid bilayers (SLBs) near neutral pH. A fluorescence quenching assay was designed by incorporating Texas Red 1,2-dihexadecanoyl-*sn*-glycero-3-phosphoethanolamine (TR-DHPE) into the SLB.[12−14,27−29] Changes in the fluorescence response of this probe were monitored by fluorescence microscopy upon Cu^{2+} binding. It was found that a 1:2 Cu^{2+}−S1P complex was formed (Figure 1a, right). Moreover, the affinity of Cu^{2+} for S1P could be strongly modulated by varying the system pH or by changing the

Received: November 4, 2018
Revised: December 14, 2018
Published: January 14, 2019

   DOI: 10.1021/acs.langmuir.8b03718
Langmuir 2019, 35, 824−830

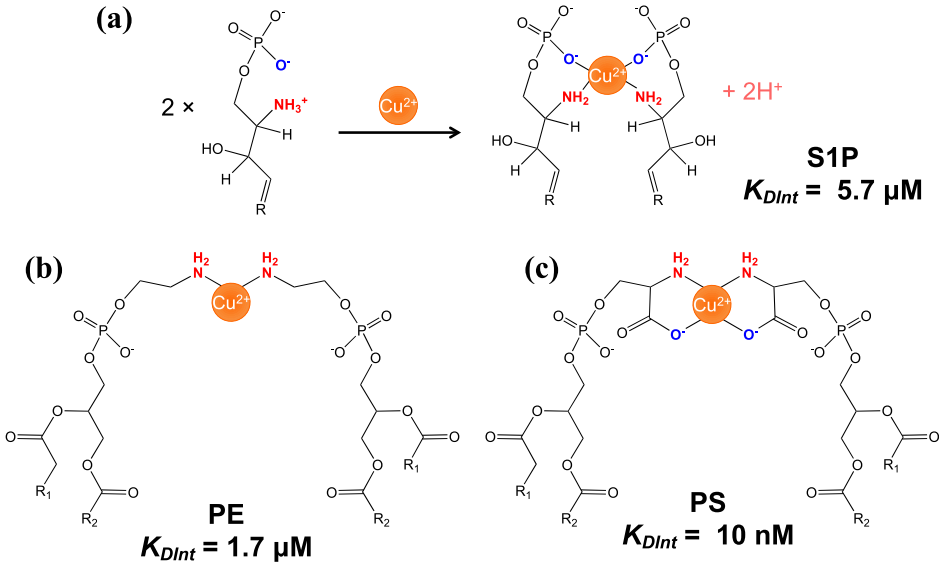

Figure 1. (a) Schematic representation for the binding of Cu^{2+} with two S1P molecules. The binding of Cu^{2+} to the amine and phosphate on two neighboring S1P lipids forms a bivalent complex with a net charge of −2. (b) The binding of Cu^{2+} to the amine groups on two neighboring PE lipids forms a bivalent complex with a net charge of 0. (c) The binding of Cu^{2+} to the amine and carboxylate groups on two neighboring PS lipids form a bivalent complex with a net charge of −2. K_{DInt} values are provided for systems with 10 mol % S1P, PE, and PS in phosphatidylcholine membranes at pH 7.4.

number density of S1P molecules in the membrane. Significantly, the binding of Cu^{2+} to S1P only occurred when the phosphate group was doubly deprotonated. These results provide insight into Cu^{2+}−S1P complex formation. Its inorganic coordination chemistry is distinct from, although reminiscent of, previously characterized Cu^{2+}−lipid complexes, such as Cu^{2+}−PS and Cu^{2+}−PE, Figure 1.[12,13,30]

RESULTS

Determining the Stoichiometry for the Binding of S1P with Cu^{2+}. In a first set of experiments, bulk fluorescence assays were used to determine the stoichiometry of binding between S1P and Cu^{2+}. Measurements were made in vesicle solutions containing 20 mol % S1P, 0.5 mol % TR-DHPE, and 79.5 mol % 1-palmitoyl-2-oleoyl-*sn*-glycero-3-phosphocholine (POPC). The vesicles were analyzed at a concentration of 0.9 mg/mL, and the corresponding structures for TR-DHPE and POPC are provided in Figure S1. The vesicles, which were formed through the extrusion process, had a diameter of 120 ± 10 nm, and the solutions contained a net concentration of 262 μM S1P. It should be noted that $CuCl_2$ was introduced both inside and outside the vesicles during extrusion. Moreover, the TR-DHPE dye, imbedded in the membrane, acted as a probe to determine if Cu^{2+} bound to S1P.[29] The dye became quenched in the presence of Cu^{2+} because of the overlap of the Cu^{2+}−S1P complex absorption band with the emission band of TR-DHPE (Figure S2). The fluorescence intensity from the vesicles was quenched rapidly at low Cu^{2+} concentrations, but the rise in F_0/F became much more gradual above 130 μM Cu^{2+} (Figure 2). The *y*-axis in the figure represents the ratio of the fluorescence intensity in the absence of Cu^{2+}, F_0, divided by the intensity, F, at each Cu^{2+} concentration plotted along the *x*-axis. The crossover region between the two linear slopes occurred when the Cu^{2+} to S1P concentration ratio was almost exactly 1:2. This ratio suggests that the complex had 1:2 Cu^{2+}−S1P stoichiometry as depicted schematically in Figure 1a. This value is identical to the 1:2 complexes that were previously

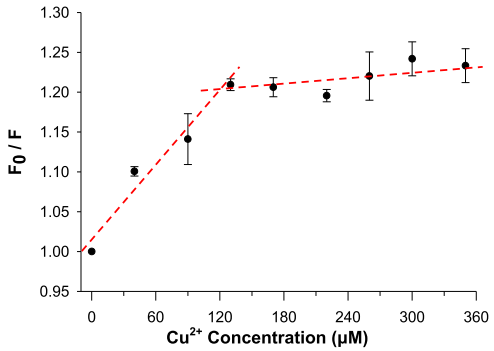

Figure 2. A Stern−Volmer plot showing the titration of 20 mol % S1P vesicles with $CuCl_2$. Lipid films were rehydrated with 10 mM tris(hydroxymethyl)aminomethane (Tris), 100 mM NaCl, and the indicated amount of Cu^{2+} as $CuCl_2$. The pH was 7.4 at all Cu^{2+} concentrations. Each data point represents an average of five independent vesicle preparations. The linear rise depicts the region in which the fluorescence is quenched before reaching a plateau (~130 μM Cu^{2+}). The red dashed lines are fits to the two linear regimes.

reported for PE and PS lipids on the addition of Cu^{2+} (Figure 1b,c, respectively).[12,13,29]

Zeta potential measurements with 20 mol % S1P vesicles were also made as a function of Cu^{2+} concentration (Table S1). These studies indicated that the surface potential was initially −19 mV and did not begin to increase until after the 1:2 complex formation was completed. Such results are consistent with the idea that the amine moieties from S1P were deprotonated on Cu^{2+} binding (Figure 1a). Moreover, the rise in zeta potential at higher Cu^{2+} concentrations suggests that the cation interacted with additional sites on the membrane at elevated concentrations, but that no further deprotonation occurred. Such additional binding probably represents weaker ion pairing interactions with the phosphate moieties.[3]

DOI: 10.1021/acs.langmuir.8b03718
Langmuir 2019, 35, 824−830

Modulation of Cu^{2+} Binding Affinity to S1P by Modulating the Lipid Charge. To determine apparent equilibrium dissociation constant values, heterogeneous assays were run using SLBs. This was done inside polydimethylsiloxane/glass microfluidic devices coated with SLBs. Buffer solutions at pH 7.4 containing a given concentration of Cu^{2+} were continuously flowed above the SLBs until the fluorescence intensities stopped changing. This ensured that equilibrium had been achieved with a known Cu^{2+} concentration in the bulk solution. In the first experiment, a two-channel microfluidic device was run with 99.5 mol % POPC and 0.5 mol % TR-DHPE in the left channel, whereas the right channel contained 10 mol % S1P, 89.5 mol % POPC, and 0.5 mol % TR-DHPE (Figure 3a). The micrograph on the left shows the two-channel device before $CuCl_2$ was introduced, whereas the micrograph on the right shows the same device after continuously flowing 25 μM $CuCl_2$ for 120 min. As can be seen from the corresponding linescan profiles (Figure 3b), the fluorescence intensity with 10 mol % S1P SLBs decreased by ~8% on exposure to Cu^{2+}, whereas the intensity for the 0 mol % S1P SLBs showed little, if any changes. Additional data were taken at a total of eight different Cu^{2+} concentrations, and these points are plotted as red triangles in Figure 4a. Also, experiments were performed at pH 5.4 and 9.4 (Figure 4a, black and green data points, respectively). The experiments at pH 5.4 corresponded to conditions where the phosphate was singly deprotonated. At pH 7.4, the phosphate was doubly deprotonated, whereas at pH 9.4, 28% of the amines were also deprotonated (see text in Supporting Information and Table S2 for details). An illustration of the corresponding protonation states is provided in Figure 4b.

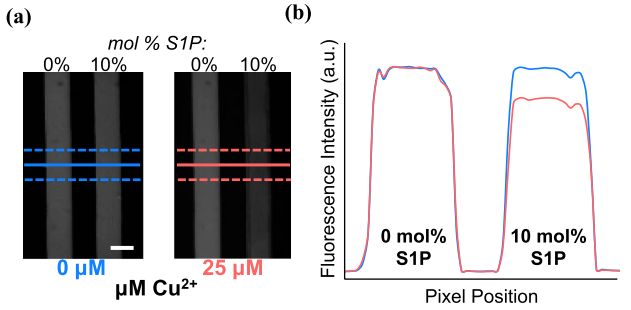

Figure 3. (a) Fluorescence micrographs of two parallel microfluidic channels containing SLBs. The left channel contained an SLB with 0 mol % S1P, whereas the right channel contained 10 mol % S1P. The two-channel image on the left shows the SLB in the absence of $CuCl_2$, whereas the right image is with 25 μM $CuCl_2$. The experiments were run at pH 7.4 in 10 mM phosphate-buffered saline (PBS) buffer with 100 mM NaCl. (b) Linescans of the fluorescence images prior to (blue line) and after (red line) exposure to $CuCl_2$. The scale bar in the bottom right corner of the first image is 100 μm in length. Control experiments were performed to verify that the SLBs were fluid under the conditions that were employed (Figure S3). Higher magnification images revealed that the bilayers appeared to be essentially continuous and relatively defect free down to the defraction limit (Figure S4).

The data at pH 5.4 were essentially flat with the concentration and could be fit to a straight line. On the other hand, the data at pH 7.4 and 9.4 were fit with Langmuir isotherms. K_{DApp} values, which were in the high nanomolar range, were abstracted from these fits and are listed in the center column of Table 1. It should also be noted that data under the most basic conditions were not taken beyond 10 μM $CuCl_2$, as the solubility limit of $Cu(OH)_2$ had been reached, as indicated by an increase in particle dispersity for Cu^{2+} in PBS buffer at pH 9.4 (Table S3). The data in Figure 4a indicated that Cu^{2+} could compete with hydronium ions for the binding sites at intermediate and high pH values but not when the pH was lowered to more acidic conditions. Moreover, having the phosphate group in the doubly deprotonated state appeared to be a requirement for Cu^{2+} binding.

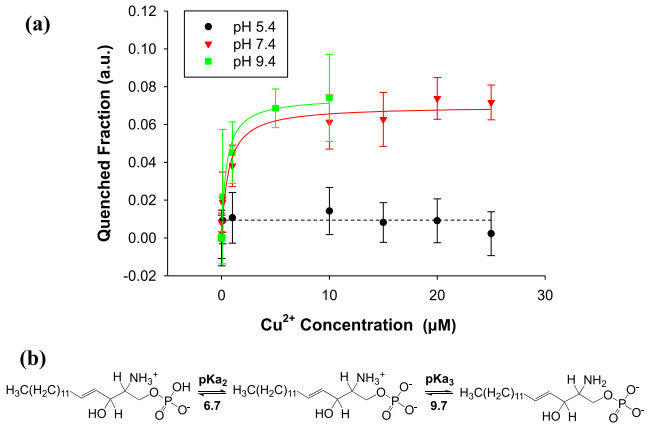

Figure 4. (a) Titration curves of SLBs containing 10 mol % S1P, 89.5 mol % POPC, and 0.5 mol % TR-DHPE with various $CuCl_2$ concentrations at three different pH values. The experiments were performed in solutions containing 10 mM PBS and 100 mM NaCl. The error bars represent standard deviations from 10 independent SLBs. The *y*-axis depicts the fraction of dye quenched by Cu^{2+} (one minus the normalized fluorescence). The solid curves represent least square fits to Langmuir isotherms at pH 7.4 and 9.4, whereas the dashed black line at pH 5.4 is a straight line fit to the data. An extended Cu^{2+} titration curve at pH 5.4 is provided in Figure S5. (b) Chemical equations for pK_{a_2} and pK_{a_3} of S1P.

Table 1. (a)K_{DApp} and K_{DInt} for Cu^{2+}–S1P in 10 mol % S1P Membranes; (b) K_{DApp} for Cu^{2+}–PA in 10 mol % S1P Membranes at pH 7.4

(a)

pH	K_{DApp} (M)	K_{DInt} (M)
5.4	N/A	N/A
7.4	$6.4 \pm 2.5 \times 10^{-7}$	5.7×10^{-6}
9.4	$4.5 \pm 0.8 \times 10^{-7}$	4.0×10^{-6}

(b)

pH	K_{DApp} (M)
7.4	$1.0 \pm 0.3 \times 10^{-4}$

Binding Measurements for Cu^{2+}–POPA. To verify that an amine group is strictly necessary for submicromolar complex formation, binding measurements were also made with 1-palmitoyl-2-oleoyl-*sn*-glycero-3-phosphate (POPA). POPA contains a phosphate group but not a free amine (Figure 5a). Figure 5b shows the binding data with Cu^{2+} at pH 7.4 using SLBs made from 10 mol % POPA, 89.5 mol % POPC, and 0.5 mol % *ortho*-rhodamine B–POPE (*o*RB–POPE) (structure provided in Figure S6). Details regarding the dye and data collection with POPA are provided in the Supporting Information section (Figure S7). POPA likely becomes doubly deprotonated on the binding of Cu^{2+}. In fact,

DOI: 10.1021/acs.langmuir.8b03718
Langmuir 2019, 35, 824–830

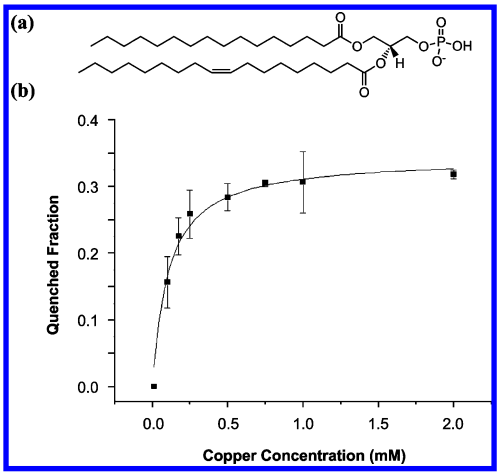

Figure 5. (a) Structure of POPA. (b) Quenched fraction of SLBs containing 10 mol % POPA, 89.5 mol % POPC, and 0.5 mol % *o*RB–DOPE at pH 7.4 versus Cu^{2+} concentration ($CuCl_2$). The experiments were performed in a buffer solution also containing 10 mM Tris and 100 mM NaCl. The error bars represent standard deviations for data collected from six independent SLBs. The *y*-axis plots the fraction of dye quenched by Cu^{2+} (one minus the normalized fluorescence). The solid curve represents a least square fit to a simple Langmuir isotherm.

PG lipids, which cannot doubly deprotonate, bind much more weakly to Cu^{2+} (Figures S8 & S9).

The data presented in Figure 5b were fit to a Langmuir isotherm, and the K_{DApp} value was determined to be 100 μM. This is in stark contrast to Cu^{2+} binding to the S1P headgroup at the same pH, which is more than 2 orders of magnitude tighter (Figure 4a, Table 1). This experiment suggests that Cu^{2+} interactions with S1P and POPA are dissimilar and consistent with the idea that the Cu^{2+}–amine interaction is of central importance for tight binding. Indeed, the binding of Cu^{2+} to POPA almost certainly represents ion pair formation between phosphate and the metal ion. By contrast, the doubly deprotonated phosphate on S1P aids in metal ion-assisted deprotonation of the amine. The latter interaction is reminiscent of the one for Cu^{2+} binding to PS, whereby a deprotonated carboxylate moiety is necessary for the Cu^{2+} to displace a proton on the amine (Figure 1c).[12,29,30]

K_{DApp} Tightens with Increasing Concentrations of S1P. As noted above, the formation of a 1:2 Cu^{2+}–S1P complex should require the loss of a proton from each of the two lipids. This leaves the surface potential unchanged. Moreover, increasing the concentration of S1P in the membrane will increase the interfacial potential. This would be expected to increase the concentration of Cu^{2+} in the double layer at constant bulk concentration. This should, in turn, lower K_{DApp} for Cu^{2+} binding. To test this idea, the affinity of Cu^{2+} for bilayers containing different densities of S1P was measured at pH 7.4 (Figure 6). These studies were conducted with 0.5 mol % TR-DHPE and a varying mixture of S1P and POPC corresponding to the other 99.5 mol % of lipids. As expected, the quenching efficiency at saturation increased with increasing concentrations of S1P in the bilayers. This is due to the decreased average distance between the Cu^{2+}–S1P complexes and TR-DHPE.[12] Indeed, at 20 mol % S1P, 8% of the fluorescence was quenched at saturation, whereas at 5.0 mol % S1P, only 3% of TR-DHPE was quenched. More significantly, the K_{DApp} value decreased with

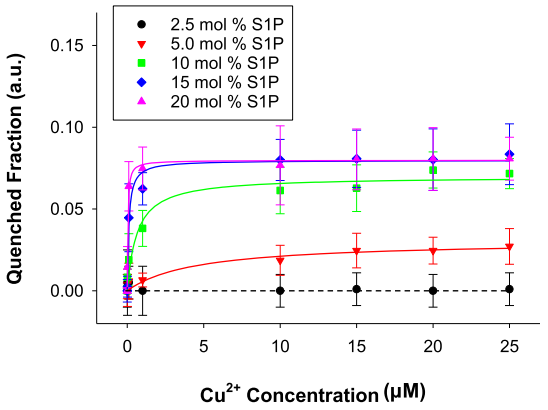

Figure 6. Quenching response of SLBs containing 2.5–20 mol % S1P. The experiments were conducted at pH 7.4. $CuCl_2$ was introduced in a buffer solution composed of 10 mM PBS and 100 mM NaCl. The geometric shapes and error bars represent data collected and averaged from over 10 independent SLBs. The *y*-axis shows the fraction of dye quenched by Cu^{2+} (one minus the normalized fluorescence). The solid lines represent fits to Langmuir isotherms. The data points for 2.5 mol % S1P are fit to a straight line.

increasing concentration of S1P in the bilayer, tightening from 4.5 μM at 5 mol % to 34 nM for bilayers containing 20 mol % S1P. This 132-fold change was the result of an increase in the surface charge, as the surface potential remained constant irrespective of the Cu^{2+} loading. The apparent tightening of the equilibrium dissociation constant should stem only in part from the higher concentration of Cu^{2+} in the double layer as the surface potential was made more negative. The remainder of the change should arise from increasing the fraction of Cu^{2+} that is bivalently, rather than monovalently bound, as will be described below.

All values of K_{DApp} extracted from Figure 6 are provided in the second column of Table 2. A Gouy–Chapman model can

Table 2. K_{DApp}, σ, ψ, and K_{DInt} for Cu^{2+}–S1P in 2.5–20 mol % S1P Membranes

mol % S1P	K_{DApp} (M)	σ (V/cm^2)	ψ (mV)	K_{DInt} (M)
2.5	N/A	-6.9×10^{-3}	−8	N/A
5.0	$4.5 \pm 2.6 \times 10^{-6}$	-1.3×10^{-2}	−15	1.4×10^{-5}
10	$6.4 \pm 2.5 \times 10^{-7}$	-2.4×10^{-2}	−28	5.7×10^{-6}
15	$1.1 \pm 0.3 \times 10^{-7}$	-3.5×10^{-2}	−40	2.5×10^{-6}
20	$3.4 \pm 0.5 \times 10^{-8}$	-4.7×10^{-2}	−50	1.7×10^{-6}

be used to convert these K_{DApp} values into intrinsic equilibrium dissociation constants, K_{DInt}. To do this, one starts with the surface charge density (σ), which can be calculated by assuming the area per lipid is 0.70 nm^2.[31] The surface potential (ψ) can then be calculated from σ by using the Grahame equation[32]

$$\sigma^2 = 2\cdot\varepsilon\cdot\varepsilon_0\cdot k\cdot T([Na^+]\, e^{-e\psi_0/k\cdot T} + [Cu^{2+}]\, e^{-2e\psi_0/k\cdot T} + [HPO_4^{2-}]\, e^{2e\psi_0/k\cdot T} + [Cl^-]\, e^{e\psi_0/k\cdot T} - [Na^+] - [Cu^{2+}] - [HPO_4^{2-}] - [Cl^-]) \quad (1)$$

where ε is the relative permittivity of water (80.2), ε_0 is the permittivity of vacuum (8.85×10^{-12} F/m), kT is the Boltzmann constant times the temperature at which the experiments were performed (298 K), e is the fundamental unit of charge (1.60×10^{-19} C), and [ion] represents the

DOI: 10.1021/acs.langmuir.8b03718
Langmuir 2019, 35, 824–830

concentrations of the respective ions in units of ions/m^3. The values for σ and ψ are listed in columns three and four of Table 2, respectively. At this point, K_{DInt} can be calculated from K_{DApp} and ψ by using the Stern equation[3]

$$K_{DInt} = K_{DApp} \times e^{-2e\psi_0/kT} \quad (2)$$

The corresponding values of K_{DInt} are provided in column five. As shown in Table 2, after correcting for changes in the surface potential, K_{DInt} only tightened by a factor of 8. As such, a factor of 16.5 from the change of K_{DApp} with S1P concentration comes from the greater surface potential (16.5 × 8 = 132). Once the surface potential portion is removed, the values of K_{DInt} can be fit to a bivalent binding model (Figure S10), which is consistent with an increase in the fraction of bivalently bound Cu^{2+} as the fraction of S1P was increased. Indeed, at sufficiently high concentrations of S1P, nascently formed 1:1 metal−lipid complexes should diffuse on the fluid membrane surface to find a second S1P molecule. This process completes the formation of the bidentate, bivalent complex. At lower mole fractions of S1P, Cu^{2+} was increasingly likely to dissociate from the lipid membrane before the 2:1 complex could be formed.

DISCUSSION

Comparisons among S1P, PS, and PE Binding to Cu^{2+}. The results described above demonstrate that Cu^{2+} binds to S1P lipids with high nM affinity, forming a 1 metal ion to 2 lipid complex. Similarly, Cu^{2+} binding to PS or PE lipids also forms a 1:2 complex. Figure 1 depicts all three cases.[12,13,29,30] Despite the fact that PE and S1P contain the same two functional moieties in their headgroups, Cu^{2+} binding is quite different in these two cases. Indeed, K_{DApp} changes quite significantly with S1P concentration (Figure 6), whereas it remains essentially unchanged when the PE density is modulated.[13] This is because the surface is continuously charged by the introduction of S1P but not by the introduction of zwitterionic PE. Moreover, metal ion-assisted deprotonation occurs when Cu^{2+} binds to S1P but not with PE. Indeed, PE needs to be deprotonated in advance for Cu^{2+} to bind. In that case, the surface potential becomes more positive on Cu^{2+} binding. There are, however, some important similarities between Cu^{2+} binding to S1P and PE. Most importantly, the value of K_{DInt} for S1P is only slightly weaker than for PE (Figure 1). As such, the phosphate group on S1P only contributes modestly to the thermodynamic stability of the complex, which implies that the amine is the dominant entity in both cases.

In some respects, S1P binding to Cu^{2+} is more similar to that of PS due to the fact that both S1P and PS give rise to metal ion-assisted deprotonation (Figure 1). Moreover, both S1P and PS bear a negative charge, and the introduction of either one into the membrane causes more Cu^{2+} to accumulate in the double layer. Also, the binding of Cu^{2+} does not lead to a change in the surface potential in either case. This means that the phosphate oxygen interaction with Cu^{2+} from S1P (blue atoms in Figure 1a) can be thought of as a reasonable substitute for the carboxylate oxygen from PS (blue atoms in Figure 1c). Nevertheless, the phosphate must be doubly deprotonated to cause metal ion-assisted deprotonation, whereas the carboxylate serves this same purpose with just a single negative charge. This difference might stem from the fact that there are two carbons in between the amine and the phosphate, whereas there is just one in between the amine and the carboxylate. Moreover, the PS also contains the same singly charged phosphate group as in S1P, and this can also help contribute to metal ion-assisted deprotonation. In fact, K_{DInt} is nearly 3 orders of magnitude tighter for the 1:2 Cu^{2+}−PS complex than it is for the 1:2 Cu−S1P complex (Figure 1). These considerations indicate that the carboxylate moiety ultimately plays a more important role in complex stabilization that does the phosphate. Indeed, metal ion-assisted deprotonation can occur at pH 5.5 with bilayers containing PS,[29] whereas the pH needs to be closer to 7.4 for Cu^{2+} binding to S1P (Figure 4).

Biological Implications of Cu^{2+}−S1P Binding. Copper ions are the third most abundant transition-metal ions in the body. They are necessary for the function of many cellular enzymes. At elevated concentrations, however, they can be toxic and may participate in the formation of reactive oxygen species, leading to cellular damage.[33−37] Such toxicity may play a role in numerous cancers and neurodegenerative diseases.[38−42] As such, copper ion homeostasis must be carefully regulated through chaperone proteins. These metallochaperones function to provide copper ions directly to specific cellular pathways so that cells are protected from intracellular copper scavangers.[43,44] Although free Cu^{2+} essentially do not exist on the inside of healthy cells, it has been suggested that transition-metal ion dishomeostasis may play a key role in disease.[43,45,46] If free Cu^{2+} do exist in such cases, then S1P would be an adventitious ligand to bind with it.

Under normal physiological conditions, the blood−brain barrier (BBB) is impermeable to copper ions. As such, movement of copper across the BBB requires specific transport systems in this case. Only when the barrier's permeability is compromised may copper ions enter the brain through passive diffusion. Although S1P is known to be a key regulator of the BBB, questions remain as to whether Cu^{2+} binding to S1P may influence the BBB. The results described herein demonstrate that Cu^{2+} can bind to S1P with sub μM affinity and can be tuned by the protonation state of the S1P molecule and its concentration in the SLB. No binding occurs at pH 5.4. Near physiological pH and above, however, the binding becomes rather tight. Overall, the rather tight binding between Cu^{2+} and S1P suggests that its role in pathophysiology should be investigated.

ASSOCIATED CONTENT

Supporting Information

The Supporting Information is available free of charge on the ACS Publications website at DOI: 10.1021/acs.langmuir.8b03718.

Materials and methods; structures of TR-DHPE and POPC; UV−vis spectra of Cu^{2+}−lipid complexes; zeta potential and size measurements of S1P−Cu^{2+} vesicles; fluorescence recovery after photobleaching images; fluorescence images of S1P SLBs under 100× magnification; amine deprotonation of S1P at pH 9.4; particle dispersity measurements of PBS with Cu^{2+} as a function of pH; binding curves for S1P versus pH expanded for pH 5.4; details on Cu^{2+} binding to POPA; Cu^{2+} binding to POPG; and fits to the bivalent binding model for S1P versus mol % (PDF)

DOI: 10.1021/acs.langmuir.8b03718
Langmuir 2019, 35, 824−830

AUTHOR INFORMATION

Corresponding Author

*E-mail: psc11@psu.edu.

ORCID

Paul S. Cremer: 0000-0002-8524-0438

Notes

The authors declare no competing financial interest.

ACKNOWLEDGMENTS

We acknowledge support from the Office of Naval Research (N00014-14-1-0792) and the National Science Foundation (CHE-1709735).

REFERENCES

(1) Haverstick, D. M.; Glaser, M. Visualization of Ca2+-Induced Phospholipid Domains. *Proc. Natl. Acad. Sci. U.S.A.* **1987**, *84*, 4475−4479.

(2) Lau, A.; McLaughlin, A.; McLaughlin, S. The Adsorption of Divalent Cations to Phosphatidylglycerol Bilayer Membranes. *Biochim. Biophys. Acta, Biomembr.* **1981**, *645*, 279−292.

(3) McLaughlin, S.; Mulrine, N.; Gresalfi, T.; Vaio, G.; McLaughlin, A. Adsorption of Divalent Cations to Bilayer Membranes Containing Phosphatidylserine. *J. Gen. Physiol.* **1981**, *77*, 445−473.

(4) McLaughlin, S. The Electrostatic Properties of Membranes. *Annu. Rev. Biophys. Biophys. Chem.* **1989**, *18*, 113−136.

(5) Shi, X.; Bi, Y.; Yang, W.; Guo, X.; Jiang, Y.; Wan, C.; Li, L.; Bai, Y.; Guo, J.; Wang, Y.; et al. Ca2+ regulates T-cell receptor activation by modulating the charge property of lipids. *Nature* **2013**, *493*, 111−115.

(6) Papahadjopoulos, D.; Portis, A.; Pangborn, W. Calcium-Induced Lipid Phase Transitions and Membrane Fusion *. *Ann. N.Y. Acad. Sci.* **1978**, *308*, 50−66.

(7) Abramson, M. B.; Katzman, R.; Gregor, H. Aqueous Dispersions Of Phosphatidylserine. Ionic Properties. *J. Biol. Chem.* **1964**, *239*, 70−76.

(8) DeSimone, J. A. The Electrostatic Contribution of Divalent Ions to the Surface Pressure of Charged Monolayers. *J. Colloid Interface Sci.* **1978**, *67*, 381−383.

(9) McLaughlin, S. G. A.; Szabo, G.; Eisenman, G. Divalent Ions and the Surface Potential of Charged Phospholipid Membranes. *J. Gen. Physiol.* **1971**, *58*, 667−687.

(10) Ohki, S.; Sauve, R. Surface Potential of Phosphatidylserine Monolayers. I. Divalent Ion Binding Effect. *Biochim. Biophys. Acta, Biomembr.* **1978**, *511*, 377−387.

(11) Papahadjopoulos, D. Surface Properties of Acidic Phospholipids: Interaction of Monolayers and Hydrated Liquid Crystals with Uni- and Bi-Valent Metal Ions. *Biochim. Biophys. Acta, Biomembr.* **1968**, *163*, 240−254.

(12) Cong, X.; Poyton, M. F.; Baxter, A. J.; Pullanchery, S.; Cremer, P. S. Unquenchable Surface Potential Dramatically Enhances Cu2+ Binding to Phosphatidylserine Lipids. *J. Am. Chem. Soc.* **2015**, *137*, 7785−7792.

(13) Poyton, M. F.; Sendecki, A. M.; Cong, X.; Cremer, P. S. Cu2+ Binds to Phosphatidylethanolamine and Increases Oxidation in Lipid Membranes. *J. Am. Chem. Soc.* **2016**, *138*, 1584−1590.

(14) Sendecki, A. M.; Poyton, M. F.; Baxter, A. J.; Yang, T.; Cremer, P. S. Supported Lipid Bilayers with Phosphatidylethanolamine as the Major Component. *Langmuir* **2017**, *33*, 13423−13429.

(15) Chalfant, C. E.; Spiegel, S. Sphingosine 1-Phosphate and Ceramide 1-Phosphate: Expanding Roles in Cell Signaling. *J. Cell Sci.* **2005**, *118*, 4605−4612.

(16) Maceyka, M.; Harikumar, K. B.; Milstien, S.; Spiegel, S. Sphingosine-1-Phosphate Signaling and Its Role in Disease. *Trends Cell Biol.* **2012**, *22*, 50−60.

(17) Strub, G. M.; Maceyka, M.; Hait, N. C.; Milstien, S.; Spiegel, S. Extracellular and Intracellular Actions of Sphingosine-1-Phosphate. *Adv. Exp. Med. Biol.* **2010**, *688*, 141−155.

(18) Hannun, Y. A.; Luberto, C.; Mao, C.; Obeid, L. M. *Bioactive Sphingolipids in Cancer Biology and Therapy*; Springer, 2015.

(19) Pyne, N. J.; Pyne, S. Sphingosine 1-Phosphate and Cancer. *Nat. Rev. Cancer* **2010**, *10*, 489−503.

(20) Santos, C. R.; Schulze, A. Sphingosine 1-phosphate signaling at the blood-brain barrier. *FEBS J.* **2012**, *279*, 2610−2623.

(21) Sato, K.; Malchinkhuu, E.; Horiuchi, Y.; Mogi, C.; Tomura, H.; Tosaka, M.; Yoshimoto, Y.; Kuwabara, A.; Okajima, F. HDL-like Lipoproteins in Cerebrospinal Fluid Affect Neural Cell Activity through Lipoprotein-Associated Sphingosine 1-Phosphate. *Biochem. Biophys. Res. Commun.* **2007**, *359*, 649−654.

(22) Karunakaran, I.; van Echten-Deckert, G. Sphingosine 1-Phosphate − A Double Edged Sword in the Brain. *Biochim. Biophys. Acta, Biomembr.* **2017**, *1859*, 1573−1582.

(23) Prager, B.; Spampinato, S. F.; Ransohoff, R. M. Sphingosine 1-Phosphate Signaling at the Blood−brain Barrier. *Trends Mol. Med.* **2015**, *21*, 354−363.

(24) Couttas, T. A.; Kain, N.; Daniels, B.; Lim, X. Y.; Shepherd, C.; Kril, J.; Pickford, R.; Li, H.; Garner, B.; Don, A. S. On the possible structural role of single chain sphingolipids Sphingosine and Sphingosine 1-phosphate in the amyloid-β peptide interactions with membranes. Consequences for Alzheimer's disease development. *Acta Neuropathol. Commun.* **2014**, *2*, 9.

(25) Watanabe, C.; Puff, N.; Staneva, G.; Seigneuret, M.; Angelova, M. I. Antagonism and Synergy of Single Chain Sphingolipids Sphingosine and Sphingosine-1-Phosphate toward Lipid Bilayer Properties. Consequences for Their Role as Cell Fate Regulators. *Langmuir* **2014**, *30*, 13956−13963.

(26) Watanabe, C.; Puff, N.; Staneva, G.; Angelova, M. I.; Seigneuret, M. Tuning of Membrane Electrostatic Properties by Single Chain Sphingolipids Sphingosine and Sphingosine-1-Phosphate: The Effect on Bilayer Dipole Potential. *Colloids Surf., A* **2015**, *483*, 181−186.

(27) Watanabe, C.; Seigneuret, M.; Staneva, G.; Puff, N.; Angelova, M. I. On the Possible Structural Role of Single Chain Sphingolipids Sphingosine and Sphingosine 1-Phosphate in the Amyloid-β Peptide Interactions with Membranes. Consequences for Alzheimer's Disease Development. *Colloids Surf., A* **2016**, *510*, 317−327.

(28) Irving, H.; Williams, R. J. P. Order of Stability of Metal Complexes. *Nature* **1948**, *162*, 746−747.

(29) Monson, C. F.; Cong, X.; Robison, A. D.; Pace, H. P.; Liu, C.; Poyton, M. F.; Cremer, P. S. Phosphatidylserine Reversibly Binds Cu2+ with Extremely High Affinity. *J. Am. Chem. Soc.* **2012**, *134*, 7773−7779.

(30) Kusler, K.; Odoh, S. O.; Silakov, A.; Poyton, M. F.; Pullanchery, S.; Cremer, P. S.; Gagliardi, L. What Is the Preferred Conformation of Phosphatidylserine−Copper(II) Complexes? A Combined Theoretical and Experimental Investigation. *J. Phys. Chem. B* **2016**, *120*, 12883−12889.

(31) White, S. H.; King, G. I. Molecular Packing and Area Compressibility of Lipid Bilayers. *Proc. Natl. Acad. Sci. U.S.A.* **1985**, *82*, 6532−6536.

(32) Israelachvili, S. Electrostatic Forces between Surfaces in Liquids. In *Intermolecular and Surface Forces*, 3rd ed.; Israelachvili, J. N., Ed.; Academic Press: San Diego, 2011; Chapter 14, pp 291−340.

(33) Esterbauer, H.; Gebicki, J.; Puhl, H.; Jürgens, G. The Role of Lipid Peroxidation and Antioxidants in Oxidative Modification of LDL. *Free Radic. Biol. Med.* **1992**, *13*, 341−390.

(34) Radi, R.; Beckman, J. S.; Bush, K. M.; Freeman, B. A. Peroxynitrite-Induced Membrane Lipid Peroxidation: The Cytotoxic Potential of Superoxide and Nitric Oxide. *Arch. Biochem. Biophys.* **1991**, *288*, 481−487.

(35) Stohs, S. J.; Bagchi, J. M. C. Oxidative Mechanisms in the Toxicity of Metal Ions. *Free Radic. Biol. Med.* **1995**, *18*, 321−336.

(36) Ząbek-Adamska, SM; Drożdż, B.; Naskalski, J. W. Dynamics of Reactive Oxygen Species Generation in the Presence of copper(II)-Histidine Complex and Cysteine. *J Lipid Res* **2013**, *60*, 565−571.

DOI: 10.1021/acs.langmuir.8b03718
Langmuir 2019, 35, 824−830

(37) Zago, M. P.; Oteiza, P. I. The Antioxidant Properties of Zinc: Interactions with Iron and Antioxidants. *Free Radic. Biol. Med.* **2001**, *31*, 266−274.
(38) Halliwell, B.; Gutteridge, J. M. Oxygen Toxicity, Oxygen Radicals, Transition Metals and Disease. *Biochem. J.* **1984**, *219*, 1−14.
(39) Lynch, S. M.; Frei, B. Mechanisms of Copper- and Iron-Dependent Oxidative Modification of Human Low Density Lipoprotein. *J. Lipid Res.* **1993**, *34*, 1745−1753.
(40) Barrera, G. Oxidative Stress and Lipid Peroxidation Products in Cancer Progression and Therapy. *Int. Scholarly Res. Not.* **2012**, *2012*, e137289.
(41) Chauhan, A.; Chauhan, V. Oxidative Stress in Autism. *Pathophysiology* **2006**, *13*, 171−181.
(42) Nair, U.; Bartsch, H.; Nair, J. Lipid Peroxidation-Induced DNA Damage in Cancer-Prone Inflammatory Diseases: A Review of Published Adduct Types and Levels in Humans. *Free Radic. Biol. Med.* **2007**, *43*, 1109−1120.
(43) Kozlowski, H.; Janicka-Klos, A.; Brasun, J.; Gaggelli, E.; Valensin, D.; Valensin, G. Copper, Iron, and Zinc Ions Homeostasis and Their Role in Neurodegenerative Disorders (Metal Uptake, Transport, Distribution and Regulation). *Coord. Chem. Rev.* **2009**, *253*, 2665−2685.
(44) Rae, T. D.; Schmidt, P. J.; Pufahl, R. A.; Culotta, V. C.; O'Halloran, T. V. Undetectable Intracellular Free Copper: The Requirement of a Copper Chaperone for Superoxide Dismutase. *Science* **1999**, *284*, 805−808.
(45) Desai, V.; Kaler, S. G. Role of Copper in Human Neurological Disorders. *Am. J. Clin. Nutr.* **2008**, *88*, 855S−858S.
(46) Waggoner, D. J.; Bartnikas, T. B.; Gitlin, J. D. The Role of Copper in Neurodegenerative Disease. *Neurobiol. Dis.* **1999**, *6*, 221−230.

DOI: 10.1021/acs.langmuir.8b03718
Langmuir 2019, 35, 824−830